Available online at www.sciencedirect.com
SCIENCE DIRECT
Journal of Molecular Catalysis A: Chemical 252 (2006) 156–162
JOURNAL OF MOLECULAR CATALYSIS A: CHEMICAL
www.elsevier.com/locate/molcata

Hydrogen oxidation reaction on microelectrodes: Analysis of the contribution of the kinetic routes

P.M. Quaino, J.L. Fernández, M.R. Gennero de Chialvo, A.C. Chialvo *

Programa de Electroquímica Aplicada e Ingeniería Electroquímica (PRELINE), Facultad de Ingeniería Química, Universidad Nacional del Litoral, Santa Fe, Argentina

Received 20 January 2006; received in revised form 22 February 2006; accepted 22 February 2006
Available online 30 March 2006

Abstract

Recent experimental studies of the hydrogen oxidation reaction (hor) on platinum microelectrodes have shown the existence of a shoulder in the steady state polarization curves. An explanation for this behavior is presented on the basis of a rigorous kinetic treatment involving the Tafel–Heyrovsky–Volmer (T–H–V) mechanism. It has been found that such behavior is due to the significant variation of the reaction rates of the Tafel–Volmer (T–V) and Heyrovsky–Volmer (H–V) routes with overpotential (η). At low η values, the T–V route dominates the kinetics of the hor, reaching values close to the maximum rate corresponding to this route. At higher η values, the contribution of the H–V route increases while that of the T–V route diminishes. On this basis, the experimental results were accurately correlated and the corresponding elementary kinetic parameters were evaluated. The contribution of the different types of microelectrodes to the improvement of the determination of the kinetic parameters for the hor is also discussed.

Keywords: Hydrogen oxidation reaction; Microelectrodes; Mechanistic analysis; Limiting current; Polarization resistance

1. Introduction

The reaction rate of the hydrogen oxidation reaction (hor) is strongly influenced by the molecular hydrogen diffusion [1–5]. A rigorous theoretical kinetic treatment of this reaction operating under the Tafel–Heyrovsky–Volmer (T–H–V) mechanism on steady state conditions has been recently derived [6]. The kinetic mechanism was solved including the hydrogen mass transport process in terms of the limiting diffusion current density (j_L). It was demonstrated that this mechanism can predict the existence of a plateau or a shoulder in the dependence of the current density (j) on overpotential (η), when the equilibrium reaction rate of the Heyrovsky step (v_H^e) is less than that of the Tafel step (v_T^e). In this conditions, at low overpotentials the reaction proceeds preferentially through the Tafel–Volmer (T–V) route and the current density can reach a maximum value j_{max}. It has been already demonstrated that $j_{max} = j_{max}^{kin} j_L/(j_{max}^{kin} + j_L)$, where $j_{max}^{kin} = 2Fv_T^e/(1-\theta^e)^2$ is the limiting kinetic current density and θ^e is the equilibrium surface coverage of the adsorbed hydrogen [6]. This behavior takes place when the surface coverage $\theta(\eta)$ tends to zero before the surface concentration of molecular hydrogen is exhausted. Then, at higher η values, the contribution of the Heyrovsky–Volmer route (H–V) increases, that of the Tafel–Volmer (T–V) route becomes negligible and finally the current density reaches the j_L value.

For the hydrogen oxidation on platinum in acid solutions, it has been demonstrated that $v_H^e < v_T^e$ [7], but the behavior described above can only be appreciated when $j_L > j_{max}^{kin}$. This condition can be obtained increasing j_L, as j_{max}^{kin} cannot be modified. Unfortunately, the experimental j_L values obtained with a rotating disc electrode (RDE) are quite low ($j_L \leq j_{max}^{kin}$) yet at the highest rotation rates (10,000 rpm), and therefore the predicted plateau cannot be observed [1–5,7]. This problem can be overcome by the use of microelectrodes, which can support very large j_L values (inversely proportional to their main dimension) [8,9]. Thus, microelectrodes are more adequate for the analysis of the Faradaic contributions in the hor. On this sense, Chen and Kucernak recently published accurate experimental steady state $j(\eta, r)$ dependences measured for the hor on hemispherical Pt microelectrodes with different radii (r) [10]. These polariza-

* Corresponding author. Tel.: +54 342 4571164x2519; fax: +54 342 4571162.
E-mail address: achialvo@fiqus.unl.edu.ar (A.C. Chialvo).

1381-1169/$ – see front matter © 2006 Elsevier B.V. All rights reserved.
doi:10.1016/j.molcata.2006.02.062

Nomenclature

C^o	concentration in the bulk solution (mol cm^{-3})
D	diffusion coefficient (cm^2 s^{-1})
F	Faraday constant (96484.6 C eq^{-1})
f	F/RT: 38.659 V^{-1} (296.15 K)
j	current density (A cm^{-2})
j_L	limiting diffusion current density (A cm^{-2})
j_{max}	maximum current density (A cm^{-2})
j_{max}^{kin}	limiting kinetic current density (A cm^{-2})
P	pressure (atm)
r	microelectrode radius
R	gas constant (8.314 J mol^{-1} K^{-1})
R_p^o	equilibrium polarization resistance (Ω cm^2)
R_p^{exp}	experimental polarization resistance (Eq. (12)) (Ω cm^2)
T	temperature (K)
v_i	reaction rate of the step i (i = V, H, T) (mol cm^{-2} s^{-1})
v_i^e	equilibrium reaction rate of the step i (i = V, H, T) (mol cm^{-2} s^{-1})
V	reaction rate (mol cm^{-2} s^{-1})
V_L	limiting diffusion reaction rate (mol cm^{-2} s^{-1})
V^{XV}	reaction rate of the VX route (X = H, T) (mol cm^{-2} s^{-1})

Greek letters

α	symmetry factor
χ	shape parameter (Eq. (10))
η	overpotential (V)
θ	hydrogen surface coverage
θ^e	hydrogen equilibrium surface coverage

tion curves clearly show the predicted behavior, which could not be correlated by the approximate model used by these authors. On this context the present work reinterprets these experimental results, on the basis of rigorous kinetic expressions derived previously for the T–H–V mechanism, with the aim of verifying the descriptive capability of this theoretical treatment [6,7].

2. Theoretical Basis

The hydrogen oxidation reaction in acid solution is:

$$H_{2(g)} \rightleftharpoons 2H^+ + 2e^- \quad (1)$$

It can be described through the Tafel–Heyrovsky–Volmer mechanism, being the adsorbed hydrogen atom H_{ad} the reaction intermediate,

$$H_{2(g)} + 2S \overset{v_T^e}{\rightleftharpoons} 2H_{ad} \quad \text{Tafel} \quad (2a)$$

$$H_{2(g)} + S \overset{v_H^e}{\rightleftharpoons} H_{ad} + H^+ + e^- \quad \text{Heyrovsky} \quad (2b)$$

$$H_{ad} \overset{v_V^e}{\rightleftharpoons} H^+ + e^- + S \quad \text{Volmer} \quad (2c)$$

where S is an adsorption site and v_i^e is the equilibrium reaction rate of the elementary step i (i = V, H, T).

2.1. Current density-overpotential dependence

The theoretical expression corresponding to the dependence $j(\eta, j_L)$ has been already derived for the case of hydrogen diffusion towards a rotating disk electrode (RDE) [6], but it can be generalized to any system in which the diffusion layer can be considered at steady state. It should be emphasized that j_L is the limiting diffusion current density, achieved when the surface concentration of molecular hydrogen is exhausted.

As there are three elementary steps and only one intermediate species, the whole reaction can be verified through two independent routes, Tafel–Volmer (T–V) and Heyrovsky–Volmer (H–V), respectively. Taking into account that in steady state the mass balance of each participant of the elementary reactions (2a)–(2c) must satisfy the corresponding mass balance of the whole reaction (1), the following relationships can be derived for the simultaneous occurrence of the two routes:

$$j = 2FV = F(v_V + v_H) = 2F(v_H + v_T) = 2F(v_V - v_T) \quad (3)$$

where $v_i = v_{+i} - v_{-i}$; i = V, H, T. V is the rate of reaction (1), v_i the rate of the step i, being v_{+i} and v_{-i} the rates of the forward and backward reaction of the step i, respectively. The corresponding expressions of v_i are (for more details see Ref. [6]):

$$v_T = v_T^e \left[\left(\frac{1-\theta}{1-\theta^e} \right)^2 \left(1 - \frac{j}{j_L} \right) - \left(\frac{\theta}{\theta^e} \right)^2 \right] \quad (4)$$

$$v_H = v_H^e \left[\left(\frac{1-\theta}{1-\theta^e} \right) \left(1 - \frac{j}{j_L} \right) e^{\alpha f \eta} - \left(\frac{\theta}{\theta^e} \right) e^{-(1-\alpha) f \eta} \right] \quad (5)$$

$$v_V = v_V^e \left[\left(\frac{\theta}{\theta^e} \right) e^{\alpha f \eta} - \left(\frac{1-\theta}{1-\theta^e} \right) e^{-(1-\alpha) f \eta} \right] \quad (6)$$

Substituting Eqs. (4)–(6) into Eq. (3) and reordering, the following equation for $j(\eta, j_L)$ is obtained,

$$\begin{aligned} j(\eta, j_L) &= \frac{(\theta/\theta^e)[v_V^e e^{\alpha f\eta} - v_H^e e^{-(1-\alpha) f\eta}] + ((1-\theta)/(1-\theta^e))[v_H^e e^{\alpha f\eta} - v_V^e e^{-(1-\alpha) f\eta}]}{\left[1/F + ((1-\theta)/(1-\theta^e))(v_H^e/j_L) e^{\alpha f\eta}\right]} \\ &= \frac{2v_H^e[((1-\theta)/(1-\theta^e)) e^{\alpha f\eta} - (\theta/\theta^e) e^{-(1-\alpha) f\eta}] + 2v_T^e[((1-\theta)/(1-\theta^e))^2 - (\theta/\theta^e)^2]}{[1/F + 2((1-\theta)/(1-\theta^e))(v_H^e/j_L) e^{\alpha f\eta} + 2((1-\theta)/(1-\theta^e))^2 (v_T^e/j_L)]} \\ &= \frac{2v_V^e[(\theta/\theta^e) e^{\alpha f\eta} - ((1-\theta)/(1-\theta^e)) e^{-(1-\alpha) f\eta}] - 2v_T^e[((1-\theta)/(1-\theta^e))^2 - (\theta/\theta^e)^2]}{[(1/F) - 2((1-\theta)/(1-\theta^e))^2 (v_T^e/j_L)]} \end{aligned} \quad (7)$$

A Langmuirian behavior has been adopted for the adsorbed reaction intermediate H_{ad}, which is justified by the very low values of θ found for this reaction [7]. It is necessary to know also the corresponding dependence $\theta(\eta, j_L)$, which can be obtained for instance rearranging the equality between the second and third members of Eq. (7) [6]:

$$\left[\left(\frac{1-\theta}{1-\theta^e}\right)\mathrm{e}^{-(1-\alpha)f\eta} - \left(\frac{\theta}{\theta^e}\right)\mathrm{e}^{\alpha f\eta}\right]\left\{v_V^e + \left(\frac{1-\theta}{1-\theta^e}\right)\frac{2F}{j_L}\left[\left(\frac{1-\theta}{1-\theta^e}\right)v_T^e v_V^e + \left(\frac{\theta}{\theta^e}\right)v_T^e v_H^e + v_V^e v_H^e\,\mathrm{e}^{\alpha f\eta}\right]\right\}$$
$$+ 2v_T^e\left[\left(\frac{1-\theta}{1-\theta^e}\right)^2 - \left(\frac{\theta}{\theta^e}\right)^2\right] + v_H^e\left[\left(\frac{1-\theta}{1-\theta^e}\right)\mathrm{e}^{\alpha f\eta} - \left(\frac{\theta}{\theta^e}\right)\mathrm{e}^{-(1-\alpha)f\eta}\right] = 0 \quad (8)$$

In Eqs. (7) and (8), α is the symmetry factor (considered the same for the Volmer and Heyrovsky steps), $f = F/RT$ and θ^e is the equilibrium surface coverage. It should be noticed that these expressions are independent of the way in which the steady state of the diffusion process is achieved (rotating disc, hemispherical diffusion, etc.). In the present case, the limiting current density on steady state corresponds to the diffusion of molecular hydrogen towards a microelectrode surface and can be described by the following Eq. [8–10],

$$j_L(r) = \frac{nFD_{H_2}C^o_{H_2}\chi_k}{r} = \frac{B}{r}\chi_k \quad (9)$$

where D_{H_2} and $C^o_{H_2}$ are the diffusion coefficient and the bulk concentration of molecular hydrogen, respectively. χ_k is a shape parameter of the microelectrode k, which depends only on the geometry of the electrode (see Table 1). This parameter is defined as the relationship between the limiting current density of a microelectrode with geometry k (j_L^k) and that of an hemispherical microelectrode (j_L^{hs}) with the same external radius (r),

$$\chi_k = \frac{j_L^k}{j_L^{hs}} \quad (10)$$

The limiting current density increases as the value of r decreases. Therefore, if microelectrodes with different radii are available, the dependence $j(\eta, j_L)$ will be evaluated through $j(\eta, r)$. The correlation of these results at constant r through Eqs. (7) and (8) will give a set of elementary kinetic parameters (v_V^e, v_H^e, v_T^e, θ^e) for each microelectrode. The coincidence of these values, calculated independently, will verify the validity of the applied kinetic treatment.

2.2. Equilibrium polarization resistance

Taking into account that the reversible potential of the hydrogen electrode reaction (HER) is perfectly defined (absence of corrosion processes) on the materials usually employed as electrocatalysts for the hor, the evaluation of the polarization resistance at equilibrium (R_p^o) can be useful for the purpose of the present work [13]. The following experimental dependence must be determined in order to obtain R_p^o,

$$\left(\frac{\partial\eta(j_L)}{\partial j}\right)^{exp}_{\eta=0} = R_p^{exp}(j_L) \quad (11)$$

$R_p^{exp}(j_L)$ can be related to the equilibrium polarization resistance by the following expression [7],

$$R_p^{exp}(j_L) = R_p^o + \frac{RT}{2F}\frac{1}{j_L} \quad (12)$$

The relationship between j_L and r given by Eq. (9) can also be used in this case to define the $R_p^{exp}(r)$ dependence for any particular microelectrode geometry. Meanwhile, R_p^o is related to the equilibrium reaction rates v_i^e by the following relationship [14],

$$R_p^o = \frac{RT}{4F^2}\left[\frac{4v_T^e + v_H^e + v_V^e}{v_V^e v_H^e + v_V^e v_T^e + v_T^e v_H^e}\right] \quad (13)$$

The values of the kinetic parameters obtained as described above can be used to calculate R_p^o from Eq. (13). Then, the resulting value can be compared to the equilibrium polarization resistance obtained from the experimental determination in order to confirm the validity and self-consistency of the proposed approach.

3. Results

The theoretical expressions described above were used for the correlation of experimental results of the hor on microelectrodes with different radii. These evaluations were carried out on accurate experimental dependences $j^{exp}(\eta, r)$ and

Table 1
Shape parameters for microelectrodes with different geometries

Microelectrode geometry	Shape parameter (χ)	Dimension
Hemisphere [8]	1	r: radius
Disc [8]	$4/\pi$	r: radius
Ring [11]	$\dfrac{\pi}{(1-(b/r))\ln[16((1+b/r)/(1-b/r))]}$; $\dfrac{b}{r} > 0.8$	r: outer radius; b: inner radius
Cone [12]	$\dfrac{4[1+q(b/r)^p]}{\pi[1+(b/r)^2]^{1/2}}$; $q = 0.3661$, $p = 1.14466$	r: basal radius; b: height

Table 2
Kinetic parameters of the hor, calculated from the regression of $j(\eta)$ of microelectrodes with different radii [10] (v_i^e in mol s^{-1} cm^{-2})

r (nm)	v_V^e	v_H^e	v_T^e	θ^e
12500	5.75×10^{-6}	1.16×10^{-8}	4.06×10^{-7}	1.98×10^{-7}
1100	1.74×10^{-6}	4.83×10^{-8}	2.05×10^{-6}	2.97×10^{-7}
450	8.29×10^{-6}	4.16×10^{-8}	1.70×10^{-6}	4.43×10^{-8}
310	2.47×10^{-6}	4.30×10^{-8}	1.16×10^{-6}	1.21×10^{-7}
36	6.03×10^{-6}	1.33×10^{-7}	6.99×10^{-6}	1.16×10^{-7}
Mean value (present work)	4.86×10^{-6}	5.56×10^{-8}	2.95×10^{-6}	1.55×10^{-7}
Standard deviation	2.7×10^{-6}	4.4×10^{-8}	2.6×10^{-6}	1.0×10^{-7}
Mean value (RDE) [7]	5.21×10^{-7}	$\sim 10^{-14}$	1.37×10^{-6}	1.46×10^{-7}

$R_p^{exp}(r)$ obtained by Chen and Kucernak [10]. They studied the hydrogen oxidation reaction employing platinum disc and hemispherical microelectrodes with radii in the range 36 nm $\leq r \leq$ 12,500 nm. These measurements were carried out in 0.1 M H_2SO_4 solutions, at 23 °C and 1 atm of hydrogen pressure ($P_{H_2}^e$) [10]. The corresponding correlations of the experimental data with the theoretical equations were done with the software Scientist Version 2.1, using a least squares minimization algorithm.

3.1. Analysis of the dependence $j^{exp}(\eta, r)$

Table 2 shows the values of the elementary kinetic parameters (v_V^e, v_H^e, v_T^e, θ^e) obtained for each microelectrode through the regression of the experimental data [10] by the use of Eqs. (7) and (8) and considering $\alpha = 0.5$. Such correlations, which are completely independent between each other, indicate that the kinetic parameters are maintained reasonably constant for different microelectrode radii (and j_L values). The fitting capability can be observed in Fig. 1, where dots indicate experimental values of the relationship (jj_L^{-1}) and lines the corresponding simulations obtained from the kinetic parameters calculated by regression (Table 2).

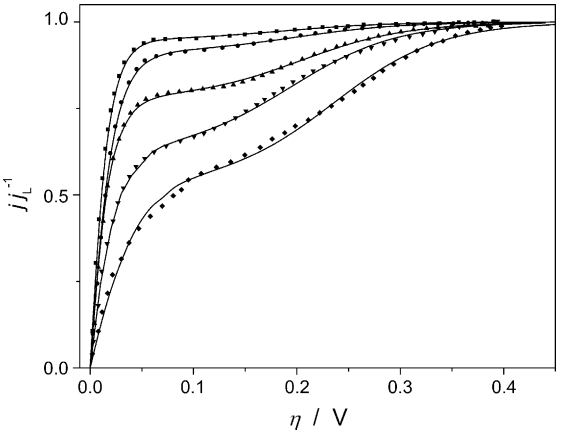

Fig. 1. Experimental (symbols) and theoretical (solid lines) $j(\eta)$ dependences of the hor on Pt microelectrodes. Experimental curves were obtained from ref. [10] and normalized with respect to the diffusion limiting currents. Radius (nm): 12,500 (■), 1100 (●), 450 (▲), 310 (▼) and 36 (♦).

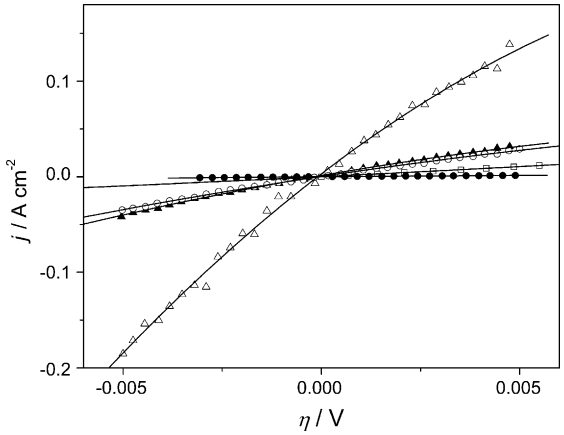

Fig. 2. $j(\eta)$ dependences near the equilibrium potential on Pt microelectrodes. Experimental curves (symbols) were obtained from ref. [10]. Radius (nm): 12,500 (●), 1100 (□), 450 (◯), 310 (▲) and 36 (△). Solid lines are correlations with a second order polynomial function, used to calculate R_p^{exp} according to Eq. (11).

3.2. Analysis of the dependence $R_p^{exp}(r)$

Starting from the experimental dependence $j^{exp}(\eta, r)$ near the equilibrium potential obtained by Chen and Kucernak [10], the values of $R_p^{exp}(r)$ were calculated. A second order polynomial was used in order to correlate $j^{exp}(\eta, r)$ near equilibrium at each r value, being the coefficient of the linear term equal to $R_p^{exp}(r)$. Fig. 2 shows the experimental results (symbols) as well as the corresponding regression (lines). The values of $R_p^{exp}(r)$ are given in Table 3.

The correlation of $R_p^{exp}(r)$ through the use of Eq. (12) allowed the evaluation of the equilibrium polarization resistance. Fig. 3 illustrates the experimental dependence $R_p^{exp}(r)$ versus $(2fj_L)^{-1}$.

Table 3
Experimental j_L and R_p values determined from $j(\eta)$ curves near the equilibrium potential on electrodes with different radii [10]

r (nm)	j_L (A cm^{-2})	$R_p^{exp}(j_L)$ (Ω cm^2)
12500	0.00433	3.102
1100	0.0387	0.493
450	0.0934	0.161
310	0.137	0.139
36	1.173	0.0314

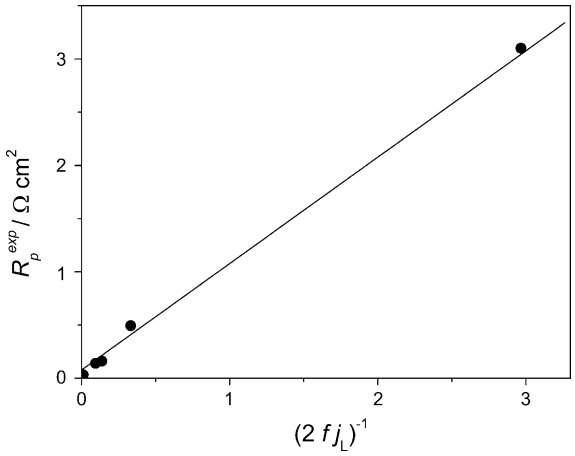

Fig. 3. (●) Experimental polarization resistance (R_p^{exp}) vs. $(2fj_L)^{-1}$ plot. (Solid line) Linear regression using Eq. (12).

The limiting diffusion current density was calculated from Eq. (9) and the product $B\chi_k$ was obtained for each microelectrode from the original work [10]. The slope of the straight line in Fig. 3 is equal to 1, which verifies Eq. (12). The value obtained for the equilibrium polarization resistance (origin ordinate) was $R_p^o = 0.077\,\Omega\,cm^2$.

4. Discussion

The present work has verified the validity of the kinetic description of the hydrogen oxidation reaction previously carried out, which predicted the existence of a plateau or a shoulder in the steady state current-potential dependence when $v_H^e < v_T^e$ [6]. This situation can be observed only if $j_L > j_{max}^{kin}$, condition that can be fulfilled with the use of microelectrodes.

The complete set of kinetic parameters corresponding to the T–H–V mechanism was evaluated starting from experimental data obtained by Chen and Kucernak [10] on platinum disc and hemispherical microelectrodes.

The quality of the correlations between theoretical and experimental data in the complete range of η (Fig. 1) is very good, fitting appropriately the shoulder region. The kinetic parameters obtained from these regressions are reported in Table 2. It should be taken into account that an independent correlation was done for each set of experimental data corresponding to the different microelectrode radii, and the resulting sets of kinetic parameters are quite similar. Furthermore, it should be noticed that the results are independently confirmed by the analysis of the other experimental results obtained in the potential region near equilibrium [10]. It can be observed in Fig. 3 that the values of $R_p^{exp}(r)$ versus $(2f\,j_L)^{-1}$ follows the straight line predicted by Eq. (12) with a slope equal to one and the origin ordinate $R_p^o = 0.077\,\Omega\,cm^2$. On the other hand, the equilibrium polarization resistance was also calculated from the mean values of the kinetic parameters illustrated in Table 2 using Eq. (13), being this value $R_p^o = 0.079\,\Omega\,cm^2$. The agreement of these values, obtained from completely different procedures and data, proves the total self-consistency of the present treatment.

All these evidences demonstrate that the kinetic expressions derived for the T–H–V mechanism are adequate to describe the hor [6]. It is interesting to compare these values with those previously reported [7], evaluated from the correlation of data obtained on a platinum RDE and also shown in Table 2. Although the experimental conditions are not exactly the same (0.5 M H_2SO_4, 30 °C [7] and 0.1 M H_2SO_4, 23 °C [10]), it should be noticed that the values of v_V^e, v_T^e and θ^e are quite similar, while v_H^e is rather different. It has been observed in the correlation of the experimental dependences $j(\eta)$ an increase in the sensibility of the parameter v_H^e as j_L increases. This sensibility is directly proportional to the difference between j_{max} and j_L. Thus, the error in the correlation of the results obtained on RDE [7] is poorly sensitive to v_H^e in the range $v_H^e < 10^{-8}$. A great number of iterations are needed in the process of convergence to the absolute minimum and the resulting value of v_H^e is rather uncertain. On the other hand, for higher j_L values such as those obtained with the microelectrodes analyzed in the present work, the sensibility of the parameter v_H^e is significantly increased. In this case, if the v_H^e value corresponding to the minimum error is modified during the fitting process, the convergence to the original value is almost immediate. Therefore, it is likely that the value $v_H^e \cong 10^{-8}$ obtained from the experimental data of Chen and Kucernak [10] is more accurate than the value $v_H^e \cong 10^{-14}$ previously reported [7].

The very low values of the equilibrium surface coverage (Table 2) are due to that the reaction intermediate of the hydrogen electrode reaction H_{ad} on platinum is the over-potential deposited hydrogen (H_{OPD}), which appears only after the surface is almost covered by the under-potential deposited hydrogen (H_{UPD}) [15]. On the other hand, the small differences between the values of the kinetic parameters calculated from each data set are probably originated in the experimental measurements. It should be taken into account that as the limiting diffusion current is increased, the experimental requirements related to absence of impurities, hydrogen saturation of the solution, absence of convection transfer, etc., are higher. Consequently, a little dispersion of the experimental results can be expected.

4.1. The competitive effect of T–V and H–V routes

In order to clarify the origin of the plateau or shoulder observed in the dependences $j(\eta)$, it is convenient to evaluate the contribution of the Tafel–Volmer (V^{TV}) and Heyrovsky–Volmer (V^{HV}) routes on the reaction rate V. Taking into account Eq. (3), it can be easily demonstrated that $V^{TV} = v_T$, $V^{HV} = v_H$ and therefore,

$$V = \frac{j}{2F} = v_T + v_H = V^{TV} + V^{HV} \tag{14}$$

Figs. 4 and 5 show the variation of the reaction rate on overpotential $V(\eta)$, as well as the contribution of each step v_i, calculated by Eqs. (4)–(6), for microelectrodes with $r = 12{,}500$ and 36 nm, respectively. The dependences of θ and the relationship between the hydrogen pressure at the surface and at the bulk ($P_{H_2}^s / P_{H_2}^e = 1 - j(\eta)/j_L$) on η [6] are also shown. It can be clearly appreciated in Fig. 4a that $V \cong V^{TV} = v_T$ for $\eta < 0.05$ V

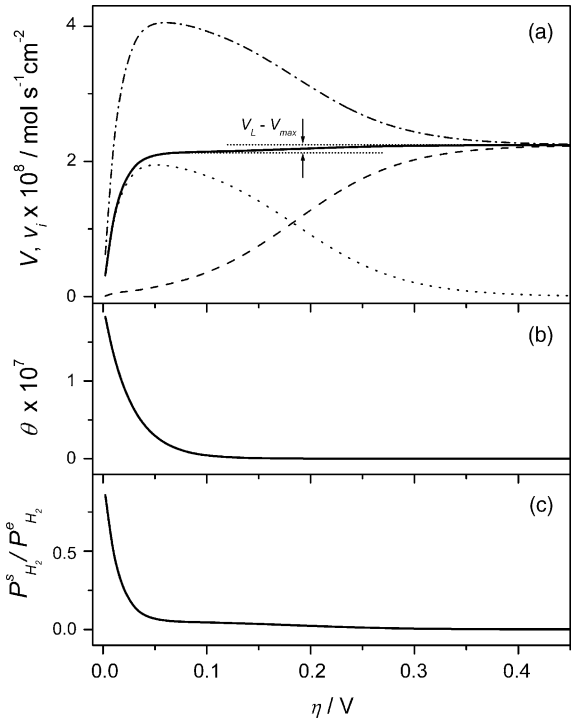

Fig. 4. Dependences of (a) Tafel (dotted line), Heyrovsky (dashed line) and Volmer (dot dashed line) step rates v_i and reaction rate V (solid line) on η, (b) θ on η, and (c) $P^s_{H_2}/P^e_{H_2}$ on η, simulated using the kinetic parameters calculated from the regression of $j(\eta)$ for $r = 12{,}500$ nm (Table 2).

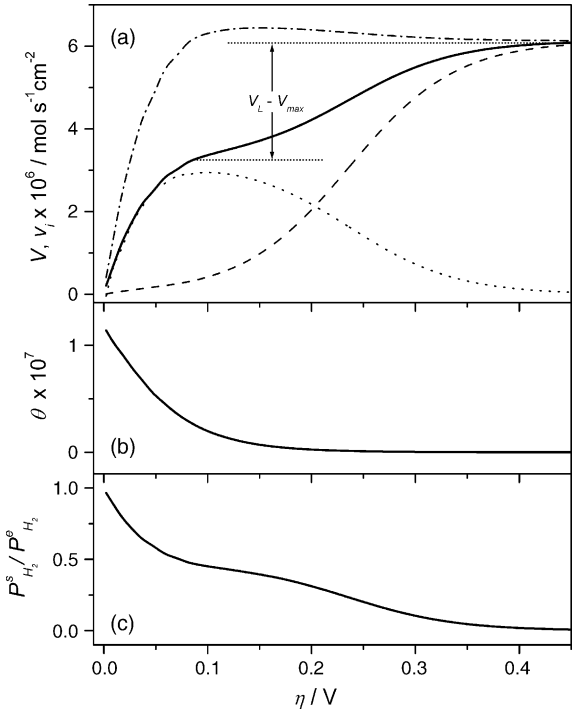

Fig. 5. Dependences of (a) Tafel (dotted line), Heyrovsky (dashed line) and Volmer (dot dashed line) step rates v_i and reaction rate V (solid line) on η, (b) θ on η and (c) $P^s_{H_2}/P^e_{H_2}$ on η, simulated using the kinetic parameters calculated from the regression of $j(\eta)$ for $r = 36$ nm (Table 2).

and also that θ and $P^s_{H_2}$ tend to zero simultaneously. The corresponding value of the maximum rate ($V^{TV}_{max} = j_{max}/2F$) is $V^{TV}_{max} = 2.13 \times 10^{-8}$ mol s^{-1} cm^{-2}, similar to that of the limiting diffusion rate $V_L = j_L/2F = 2.24 \times 10^{-8}$ mol s^{-1} cm^{-2}. As this difference is quite small, the shoulder in $V(\eta)$ cannot be observed in Fig. 4a. Conversely for the microelectrode with $r = 36$ nm (Fig. 5), $V^{TV}_{max} = 3.25 \times 10^{-8}$ mol s^{-1} cm^{-2} and $V_L = 6.08 \times 10^{-8}$ mol s^{-1} cm^{-2}. In this case, the difference is significant and consequently, when the overpotential reaches the region where $\theta \to 0$ (Fig. 5b), the surface concentration of molecular hydrogen is still high (Fig. 5c), being $P^s_{H_2} \cong 0.25 P^e_{H_2}$. On the other hand, although in both cases (Figs. 4 and 5), it can be observed a slow increase of V^{HV} at low η, the main difference between them is the value of V^{TV}_{max}, which explains the existence of the shoulder in the dependence $V(\eta)$.

4.2. Criteria for the microelectrode selection

It should be of interest to analyze the effect of the geometry and dimension of the microelectrode on the kinetic study of the hydrogen oxidation reaction. In this sense, it is important to obtain an appropriate difference between j_{max} and j_L because it has direct influence on the accuracy of the calculation of the kinetic parameters, particularly v^e_H.

Fig. 6 shows the dependences of j_L and j_{max} on the electrode radius for a disc and a ring platinum microelectrode, the last one with two different ratios b/r (0.98 and 0.95). It can be observed that j_{max} deviates from j_L for the disc electrode when $r < 1$ μm, while for the ring the deviation takes place when $r < 30$ μm for $b/r = 0.98$ and $r < 10$ μm for $b/r = 0.95$ (ring thickness < 50 nm). The difference between j_{max} and j_L becomes significant when $r < 0.5$ μm for the disc, meanwhile for the ring the corresponding values are $r < 10$ μm ($b/r = 0.98$) and $r < 5$ μm ($b/r = 0.95$). Thus, it should be possible to reach the same level of accuracy in the calculation of the kinetic parameters as that obtained in the present work through the use of a ring microelectrode with a radius more than one order of magnitude greater. Considering that several straightforward methods for preparation of

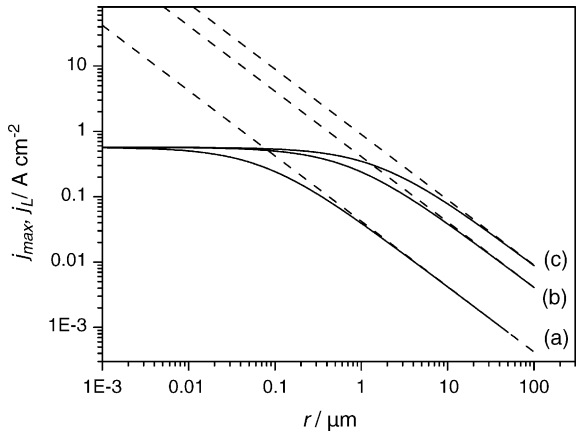

Fig. 6. Dependence of j_{max} (solid line) and j_L (dashed line) on the outer radius (r) for a ring microelectrode with $b/r = 0.98$ (c) and 0.95 (b) and for a disc microelectrode (a).

ring microelectrodes with these dimensions have been reported [16,17], the use of this type of electrode to perform kinetic studies turns to be an attractive alternative.

5. Conclusion

The experimental behavior of the hydrogen oxidation reaction on platinum microelectrodes has been explained on the basis of a rigorous kinetic treatment involving the Tafel–Heyrovsky–Volmer mechanism. It has been found that such behavior is due to the significant variation of the reaction rates of the Tafel–Vomer and Heyrovsky–Volmer routes with overpotential. On this basis, the experimental results could be accurately correlated and the corresponding elementary kinetic parameters were evaluated with a high degree of confidence. The convenience of the use of microelectrodes was demonstrated, due to the significant effect of the limiting diffusion current density on the accuracy of the calculation of the kinetic parameters.

Acknowledgements

This work was supported by Agencia Nacional de Promoción Científica y Tecnológica (ANPCyT), Consejo Nacional de Investigaciones Científicas y Técnicas (CONICET) and Universidad Nacional del Litoral.

References

[1] N.M. Markovic, B.N. Grgur, P.N. Ross, J. Phys. Chem. B 101 (1997) 5405–5413.
[2] G. Bronoel, E. Museux, G. Leclercq, L. Leclercq, N. Tassin, Electrochim. Acta 36 (1991) 1543–1547.
[3] V.S. Bagotsky, N.V. Osetrova, J. Electroanal. Chem. 43 (1973) 233–249.
[4] F. Ludwig, R.K. Sen, E. Yeager, Sov. Electrochem. 13 (1977) 717–723.
[5] J.X. Wang, S.R. Brankovic, Y. Zhu, J.C. Hanson, R.R. Adzic, J. Electrochem. Soc. 150 (2003) A1108–A1117.
[6] M.R. Gennero de Chialvo, A.C. Chialvo, Phys. Chem. Chem. Phys. 6 (2004) 4009–4017.
[7] P.M. Quaino, M.R. Gennero de Chialvo, A.C. Chialvo, Phys. Chem. Chem. Phys. 6 (2004) 4450–4455.
[8] A.J. Bard, L.R. Faulkner, Electrochemical Methods: Fundamental and Applications, second ed., John Wiley & Sons, New York, 2001, p. 176.
[9] B.R. Scharifker, J.O'M. Bockris, in: B.E. Conway, R. White (Eds.), Modern Aspects of Electrochemistry, vol. 22, Plenum Press, New York, 1992, pp. 467–519.
[10] S. Chen, A. Kucernak, J. Phys. Chem. B 108 (2004) 13984–13994.
[11] A. Szabo, J. Phys. Chem. 91 (1987) 3108–3111.
[12] C.G. Zoski, M.V. Mirkin, Anal. Chem. 74 (2002) 1986–1992.
[13] J.L. Fernández, M.R. Gennero de Chialvo, A.C. Chialvo, Phys. Chem. Chem. Phys. 5 (2003) 2875–2880.
[14] M.R. Gennero de Chialvo, A.C. Chialvo, J. Electroanal. Chem. 415 (1996) 97–106.
[15] G. Jerkiewicz, Prog. Surf. Sci. 57 (1998) 137–186.
[16] Y. Lee, A.J. Bard, Anal. Chem. 74 (2002) 3626–3633.
[17] P. Liljeroth, C. Johans, C.J. Slevin, B.M. Quinn, K. Kontturi, Electrochem. Commun. 4 (2002) 67–71.